



## Air–sea CO<sub>2</sub> exchange in the Baltic Sea—A sensitivity analysis of the gas transfer velocity

Lucía Gutiérrez-Loza <sup>a,\*</sup>, Marcus B. Wallin <sup>b</sup>, Erik Sahlée <sup>a</sup>, Thomas Holding <sup>c</sup>, Jamie D. Shutler <sup>c</sup>, Gregor Rehder <sup>d</sup>, Anna Rutgersson <sup>a</sup>

<sup>a</sup> Department of Earth Sciences, Uppsala University, Uppsala, Sweden

<sup>b</sup> Department of Aquatic Sciences and Assessment, Swedish University of Agricultural Sciences, Uppsala, Sweden

<sup>c</sup> Centre for Geography and Environmental Science, University of Exeter, Exeter, UK

<sup>d</sup> Department of Marine Chemistry, Leibniz Institute for Baltic Sea Research Warnemuende, Rockstock, Germany

### ARTICLE INFO

#### Keywords:

Air–sea exchange  
Transfer velocity parametrization  
CO<sub>2</sub> exchange  
Baltic sea

### ABSTRACT

Air–sea gas fluxes are commonly estimated using wind-based parametrizations of the gas transfer velocity. However, neglecting gas exchange forcing mechanisms – other than wind speed – may lead to large uncertainties in the flux estimates and the carbon budgets, in particular, in heterogeneous environments such as marginal seas and coastal areas. In this study we investigated the impact of including relevant processes to the air–sea CO<sub>2</sub> flux parametrization for the Baltic Sea. We used six parametrizations of the gas transfer velocity to evaluate the effect of precipitation, water-side convection, and surfactants on the net CO<sub>2</sub> flux at regional and sub-regional scale. The differences both in the mean CO<sub>2</sub> fluxes and the integrated net fluxes were small between the different cases. However, the implications on the seasonal variability were shown to be significant. The inter-annual and spatial variability were also found to be associated with the forcing mechanisms evaluated in the study. In addition to wind, water-side convection was the most relevant parameter controlling the air–sea gas exchange at seasonal and inter-annual scales. The effect of precipitation and surfactants seemed negligible in terms of the inter-annual variability. The effect of water-side convection and surfactants resulted in a reduction of the downward fluxes, while precipitation was the only parameter that resulted in an enhancement of the net uptake in the Baltic Sea.

### 1. Introduction

The exchange of CO<sub>2</sub> between the ocean and the atmosphere is an essential part of the global carbon cycle. During the last decades, great efforts have been made to understand and quantify the air–sea CO<sub>2</sub> exchange as it may represent an improvement to our knowledge about current and future climate. The global ocean is, on average, a net sink of anthropogenic CO<sub>2</sub> (Le Quééré et al., 2017; Friedlingstein et al., 2019; Woolf et al., 2019). However, accounting for the temporal and spatial variability of the air–sea gas exchange remains to be a challenge (Shutler et al., 2019). This is particularly true for heterogeneous environments such as coastal and marginal seas (Borges et al., 2005; Legge et al., 2020).

Marginal seas are highly active and dynamical regions in biogeochemical terms. These regions represent around 7% of the total ocean surface and less than 0.5% of the ocean volume (Gattuso et al., 1998; Chen et al., 2003). Nevertheless, their contribution per surface area to the global carbon system is disproportionately large when compared to

the open ocean (Cai et al., 2006; Lee et al., 2011; Laruelle et al., 2010). The high heterogeneity and complexity of the coastal regions, as well as the limited data availability, makes it difficult to constrain regional carbon budgets. In order to address such limitations, studies focusing on the comprehension of local and regional processes modulating the air–sea gas exchange are necessary. From a global perspective, marginal seas at temperate (30°–60°) and high (60°–90°) latitudes are described as net sinks of atmospheric carbon (Borges et al., 2005; Laruelle et al., 2010; Roobaert et al., 2019).

The Baltic Sea is a marginal sea in Northern Europe and stretches from 54°N to 66°N. For several decades, the Baltic Sea has been the subject of successful and interdisciplinary research (e.g., Meier et al., 2014). It is considered as one of the most extensively studied marginal seas in the world (Thomas et al., 2010). The spatio-temporal variability of carbon system elements in the Baltic Sea has been addressed in several studies (e.g., Thomas and Schneider, 1999; Rutgersson et al., 2008; Omstedt et al., 2009; Rutgersson et al., 2009; Wesslander et al.,

\* Corresponding author.

E-mail address: [lucia.gutierrez\\_loza@geo.uu.se](mailto:lucia.gutierrez_loza@geo.uu.se) (L. Gutiérrez-Loza).

<https://doi.org/10.1016/j.jmarsys.2021.103603>

Received 24 November 2020; Received in revised form 4 June 2021; Accepted 11 June 2021

Available online 17 June 2021

0924-7963/© 2021 The Authors.

Published by Elsevier B.V. This is an open access article under the CC BY-NC-ND license

(<http://creativecommons.org/licenses/by-nc-nd/4.0/>).

2010; Schneider and Müller, 2018). In the central Baltic Sea, the largest region of the Baltic Sea, a strong spring bloom usually around the beginning of April leads to nitrate depletion already in May, accompanied by a strong drop in the CO<sub>2</sub> partial pressure (pCO<sub>2</sub>) from values close to equilibrium with the atmosphere to well below 200 μatm. This is followed by a phase of relatively stable pCO<sub>2</sub>, with upper water production mainly fuelled by organic matter mineralization. Later in summer, periods of enhanced solar radiation under calm conditions trigger a second bloom period dominated by nitrogen-fixing cyanobacteria (Schneider and Müller, 2018). In particular, the latter can strongly vary in intensity between different years (Schneider et al., 2014), so that the lowest annual pCO<sub>2</sub> values can be observed either at the end of the spring or late summer bloom. Mixed layer deepening and mixing with deeper water masses enriched in inorganic carbon by mineralization lead to high pCO<sub>2</sub> values of up to 600 μatm in fall, slowly decaying over winter due to air–sea exchange, reaching near atmospheric equilibrium conditions again before the onset of the next production period. Even though the seasonal variability of oceanic pCO<sub>2</sub> in the region is – to great extent – well understood, large uncertainties are still associated to the air–sea CO<sub>2</sub> flux estimates.

Several approaches have been used to quantify air–sea CO<sub>2</sub> fluxes in the Baltic Sea, yet no consensus has been reached from these results. Following a mass balance approach, Thomas et al. (2010) concluded that the Baltic Sea is a net sink of CO<sub>2</sub> at a rate of –2.28 TgC yr<sup>–1</sup>, while Kuliński and Pempkowiak (2011) estimated a total net CO<sub>2</sub> emission of 1.05 TgC yr<sup>–1</sup> to the atmosphere. Results from a fully coupled physical-biogeochemical model (Omstedt et al., 2009) showed that before the industrialization era the Baltic Sea was a net source of CO<sub>2</sub> to the atmosphere, while present-day Baltic Sea has become both a sink and a source of CO<sub>2</sub> due to an increased seasonal variability of the CO<sub>2</sub> partial pressure in seawater. Using the model of Omstedt et al. (2009), Norman et al. (2013b) found the Baltic Sea to be a net sink of –0.20 mol m<sup>–2</sup> yr<sup>–1</sup> – on average – using data from 1960 to 2009. In contrast, Parard et al. (2017) presented climatological maps of air–sea CO<sub>2</sub> fluxes over the Baltic Sea using estimates of pCO<sub>2</sub> in seawater derived from satellite images. Their results suggest that the Baltic Sea is a small net source of CO<sub>2</sub> (1.2 mmol m<sup>–2</sup> d<sup>–1</sup>), with stronger contributions from the Southern and Central Basins compared to the northern regions.

The exchange of CO<sub>2</sub> across the air–sea interface is controlled by the difference between the oceanic and atmospheric concentration of CO<sub>2</sub> (ΔC), and by the efficiency of the transfer processes often expressed in terms of the gas transfer velocity (*k*). Wind-based parametrizations of the gas transfer velocity which are commonly used for open ocean conditions (e.g. Wanninkhof and McGillis, 1999; Weiss et al., 2007; Wanninkhof, 2014) are not always adequate for coastal environments. In the Baltic Sea, concentrations of CO<sub>2</sub> in the seawater (*C<sub>w</sub>*) present a large spatial and seasonal variability caused by physical forcings and biogeochemical processes at local and regional scales (Wesslander et al., 2010; Parard et al., 2014). These physical and biochemical mechanisms also play a key role on modulating the efficiency of the gas transfer across the interface. Therefore, resolving the variability of the sea surface CO<sub>2</sub> concentration, and including the relevant mechanisms in the gas transfer velocity parametrizations is essential to accurately describe the air–sea fluxes and their contribution to the regional carbon budgets.

Water-side convection has been shown to be an important factor affecting the diurnal and seasonal cycles of the air–sea CO<sub>2</sub> fluxes in the Baltic Sea due to enhanced turbulence at the sea surface and increased vertical transport caused by the thermal convection (Rutgersson and Smedman, 2010; Norman et al., 2013b). Biologically-derived surfactants can cause a reduction on air–sea CO<sub>2</sub> gas exchange through turbulence suppression at the sea surface. The effect of surfactants has been shown to be relevant both in coastal regions (Pereira et al., 2016) and open ocean (Pereira et al., 2018). Meanwhile, precipitation is recognized to increase the carbon sink both at regional and global

scales by altering the physical and chemical characteristics of the ocean surface (Ashton et al., 2016). In the Baltic Sea, other processes not addressed in this study, such as upwelling events (Norman et al., 2013a), sea state, and ice coverage (Löffler et al., 2012) might be relevant and not often accounted for in the current flux estimates.

In this study we investigated the impact of including relevant parameters such as wind, precipitation, water-side convection and surfactants on the gas transfer velocity parametrization for air–sea CO<sub>2</sub> flux (*F*CO<sub>2</sub>) calculations in the Baltic Sea. Using a sensitivity analysis of the gas transfer velocity and the corresponding air–sea CO<sub>2</sub> fluxes, we aim to highlight the importance of different forcing mechanisms on the regional budgets and to address the temporal and spatial variability of the fluxes in the Baltic Sea. To perform this sensitivity analysis, we used the FluxEngine software (Shutler et al., 2016; Holding et al., 2019) as a tool to calculate the air–sea CO<sub>2</sub> fluxes and net integrated CO<sub>2</sub> fluxes at a sub-regional and regional scales. We are aware of the large uncertainties associated to the fluxes, and therefore, we do not intend to present accurate estimations of the air–sea CO<sub>2</sub> fluxes in the Baltic Sea, but rather investigate the net impact of the forcing mechanisms. The study is applicable and relevant for other coastal areas and inland seas.

## 2. Theory

### 2.1. Air–sea gas exchange

The air–sea gas exchange of slightly soluble gases – such as CO<sub>2</sub> – can be defined as a function of the gas transfer velocity and the concentration difference between the top and the bottom of the aqueous mass boundary layer—the layer occupying the upper 10–200 μm of the ocean where molecular diffusion controls the vertical transport. Assuming that the concentration in the water surface is in chemical equilibrium with the bulk air above it, it is possible to express the flux as,

$$F = k(C_w - \alpha C_a), \quad (1)$$

where *F* (g m<sup>–2</sup> s<sup>–1</sup>) is the flux across the interface; by convention, the flux is positive (upward flux) when the transport occurs from the ocean to the atmosphere. Negative values of the flux (downward flux) refer to transport from the atmosphere to the ocean. The transfer velocity, *k* (m s<sup>–1</sup>), represents the efficiency of the transport associated to the turbulent processes near the surface. The concentration difference is given by the concentrations of the gas in the seawater (*C<sub>w</sub>*, g m<sup>–3</sup>) and in the air (*C<sub>a</sub>*, g m<sup>–3</sup>), and *α* is the dimensionless Ostwald solubility coefficient.

Different expressions of the bulk model exist for air–sea gas flux calculations as a function of the gas concentration (i.e. Eq. (1)), partial pressure, or fugacity. The rapid model approach (see Woolf et al., 2016) is a representation of the bulk model that takes into account vertical temperature gradients in the oceanic boundary layer, and is expressed as,

$$F = k(\alpha_w f_w - \alpha_s f_a), \quad (2)$$

where the concentration of CO<sub>2</sub> is given by the product of the CO<sub>2</sub> solubility (*α*, g m<sup>–3</sup> μatm<sup>–1</sup>) and its fugacity (*f*, μatm<sup>–1</sup>). The subscripts indicate the values in the bulk seawater (*w*), in the air (*a*), and in the air–sea interface (*s*).

The use of bulk methods for flux calculations (i.e. Eqs. (1) and (2)) entail large uncertainties to the estimates at regional and global scales. The main sources of the uncertainties are usually associated with the sparseness of data and with the intrinsic uncertainties of the gas transfer velocity parametrizations (Woolf et al., 2019). In order to constrain the flux estimates, data accounting for the variability of physical, biological, and chemical processes that control the distribution of CO<sub>2</sub>, as well as improved understanding of the mechanisms involved in air–sea gas exchange are necessary.

## 2.2. Gas transfer velocity

The gas transfer velocity represents the efficiency of the transfer processes across the air–sea interface. The efficiency of the exchange is inversely proportional to the total resistance exerted at the interface. For slightly soluble gases (like CO<sub>2</sub>), the resistance to the flux occurs almost entirely in the water phase. Therefore, turbulent processes in the oceanic boundary layer are of particular relevance for the air–sea CO<sub>2</sub> exchange. A general expression of the transfer velocity,  $k$ , can be written as,

$$k = aSc^{-n}f(Q, L, \nu), \quad (3)$$

where  $a$  is a proportionality constant often derived empirically and  $f(Q, L, \nu)$  is a function that describes the characteristics of the aqueous boundary layer in terms of a velocity scale ( $Q$ ), a length scale ( $L$ ) and the kinematic viscosity of the water ( $\nu$ ). The Schmidt number ( $Sc = \nu/D$ ) is the ratio between the kinematic viscosity of the water and the diffusion coefficient, and  $n$  is the Schmidt number exponent (e.g. Esters et al., 2017). The Schmidt number is characteristic of each individual gas, therefore, it is useful when comparing transfer velocities of different gases; additionally,  $Sc$  is temperature – and to a lesser extent – salinity-dependent, thus, essential when comparing  $k$  values under different conditions. A common practice is to use normalized values of the gas transfer velocity ( $k_{660}$ ) such that,

$$k_{660} = k(660/Sc)^{-1/2}, \quad (4)$$

where  $Sc = 660$  corresponds to the Schmidt number of CO<sub>2</sub> at 20°C for seawater ( $S = 35\text{‰}$ ), and  $Sc$  represents the value at the *in-situ* temperature and salinity conditions of any given gas.

Wind is the largest source of kinetic energy to the upper ocean. It can be associated – directly or indirectly – with most of the turbulent processes that control the air–sea gas exchange. Additionally, wind speed is a widely available parameter and most transfer velocity parametrizations are, therefore, expressed as a function of the wind speed (e.g. Wanninkhof and McGillis, 1999; Nightingale et al., 2000; Weiss et al., 2007; Wanninkhof, 2014). Some of these wind-based parametrizations have shown consistent estimates of air–sea fluxes at global scales, for example, those fitted to be in agreement with the transfer velocities determined from the global oceanic uptake of <sup>14</sup>C (e.g. Wanninkhof, 2014). However, using such parametrizations for flux calculations at regional scales might lead to large uncertainties (Woolf et al., 2019). Hence, other physical processes should be taken into consideration when calculating the air–sea gas exchange. Sea state, bubbles, surfactants, ice, and water-side convection are processes that might be relevant at regional scales in coastal environments. The relevance of these processes as forcing mechanisms can only be assessed based on local and regional studies.

## 3. Methodology

### 3.1. Study area

The Baltic Sea is a brackish semi-enclosed basin connected solely to the North Sea through the Danish Straits. The carbon system in the Baltic Sea is highly dynamical as most of its key elements present strong seasonal and latitudinal variability. In addition to the complex biogeochemical system, physical features play a key role on the distribution of nutrients and carbon in the region. Vertical and horizontal salinity gradients are caused by the limited water exchange with the open ocean in the Southwest and the large freshwater inflow in the Northern regions where river runoff ( $15,000 \text{ m}^3 \text{ s}^{-1}$ , Bergström and Carlsson (1994)) represents an important source of nutrients and carbon. Light availability and stratification have a constraining effect on biological processes.

The heterogeneity of the biogeochemical, hydrographical, and physical characteristics along the Baltic Sea makes it difficult to assess

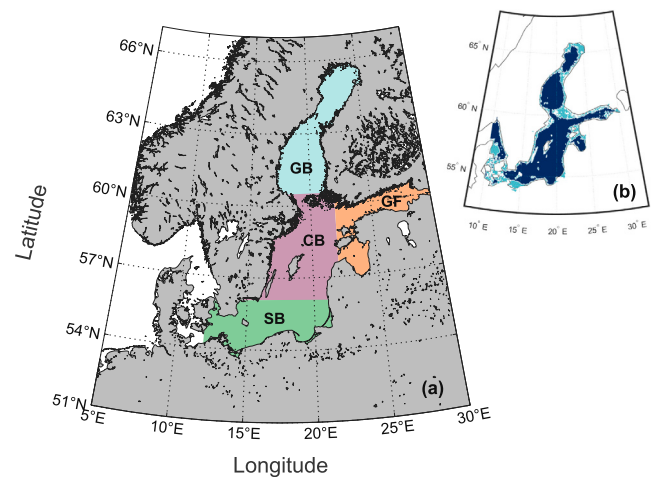


Fig. 1. Map of the Baltic Sea. In (a) the colours indicate the defined sub-regions of the Baltic Sea used in this study: Gulf of Bothnia (GB) in blue, Gulf of Finland (GF) in orange, Central Basin (CB) in pink, and Southern Basin (SB) in green. In (b) areas with depths smaller than 20 m are shown in light blue (coastal regions) and the rest in dark blue (open sea regions).

the air–sea interaction processes in the region as a whole. Parard et al. (2016) suggested to divide the Baltic Sea into four sub-regions (Fig. 1a) according to bathymetric and geographical features: The Gulf of Bothnia (GB) in the northern-most region; Gulf of Finland (GF) to the East; Central Basin (CB); and Southern Basin (SB). Additionally, we defined the coastal regions as the areas with depths smaller than 20 m (Schernewski and Wielgat, 2004), the rest was considered as open sea (Fig. 1b).

### 3.2. Input data

We used three years of data (2009–2011) from different sources for the air–sea CO<sub>2</sub> exchange and budget calculations. The period was chosen based on data availability, particularly, simultaneous surface pCO<sub>2</sub> data and high resolution wind speed over the entire Baltic Sea. An overview of each dataset is presented in this section.

Monthly atmospheric dry mole fractions of CO<sub>2</sub> ( $x_a$ , ppm) were calculated according to Rutgersson et al. (2009) using a simplified expression that considers the global trend, the natural seasonal cycle, and the anthropogenic contributions of CO<sub>2</sub>,

$$x_a = x_{trend} + x_{anthropogenic} + x_{natural}. \quad (5)$$

The global trend represents the background concentration derived from measurements in the North Sea during 1993–2005,

$$x_{trend} = 1.824a + 0.005t - 3278.2, \quad (6)$$

where  $a$  is time in years and  $t$  is the day number. The latitudinal distribution of the atmospheric CO<sub>2</sub> was accounted for within the  $x_{anthropogenic}$  and  $x_{natural}$  terms as suggested by Norman et al. (2013b),

$$x_{anthropogenic} = -0.79l + 53, \quad (7)$$

with  $l$  representing the latitude and,

$$x_{natural} = A_a \sin(2\pi/365.25(t - \theta_a)) + A_s \sin(4\pi/365.25(t - \theta_s)), \quad (8)$$

where  $A_a = 0.096l + 1.5$  and  $A_s = -0.033l + 1.5$  are the annual and semi-annual harmonics, respectively, and  $\theta_a = 1.6l + 1600$  and  $\theta_s = -0.8l + 48$  correspond to the phases.

We used existing maps of pCO<sub>2</sub> (in  $\mu\text{atm}$ ) in the seawater derived from remote sensing data as described in Parard et al. (2016, 2017). Sub-skin sea surface temperatures (SST) associated to the pCO<sub>2</sub> values were also obtained from Parard et al. (2016, 2017). The maps were

generated using self-organizing map classifications along with class-specific linear regressions (SOMLO methodology) to estimate monthly values of  $p\text{CO}_2$  for the Baltic Sea. A detailed description of the SOMLO methodology can be found in Sasse et al. (2013) and Parard et al. (2015).

Reanalysis wind speed ( $U_{10}$ ,  $\text{m s}^{-1}$ ) data from the New European Wind Atlas (NEWA) was used. NEWA is a free, web-based application developed, owned and operated by the NEWA consortium (<https://map.neweuropeanwindatlas.eu/>); they use data from ECMWF Reanalysis 5th Generation (ERA5) for the wind forcing (Hersbach et al., 2020), and OSTIA (The Operational Sea Surface Temperature and Sea Ice Analysis) products for sea surface temperature and ice (Donlon et al., 2012). The wind data had a 30-min temporal resolution and  $3 \times 3$  km spatial resolution. The second and third moments of the wind speed were calculated using the original 30-min data. The wind speed and its statistical moments were averaged to monthly values and used for transfer velocity calculations. Skin temperature,  $T_{skin}$  (in K), was also retrieved from NEWA with a 30-min temporal resolution and  $3 \times 3$  km spatial grid. The foundation temperature,  $T_{fnd}$  (i.e. sub-surface temperature), required in the rapid model approach (see Section 2.1), was derived from  $T_{fnd} = T_{skin} + \Delta T$  considering a cool skin difference of  $\Delta T = 0.17$  K (Donlon et al., 2002).

We used monthly atmospheric pressure at the sea surface ( $P$ , mbar) from NCEP Reanalysis, and precipitation rates ( $R_n$ ,  $\text{mm d}^{-1}$ ) from CMAP precipitation data, both datasets provided by the NOAA/OAR/ESRL PSD, Boulder, Colorado, USA, from their website at <https://www.esrl.noaa.gov/psd/> (Xie and Arkin, 1997). Monthly data of sea surface salinity (in PSU), mixed layer depth (in m), and fraction of sea ice coverage were taken from the Baltic Sea physical reanalysis product provided by CMEMS (Copernicus Marine Environment Monitoring System) (Von Schuckmann et al., 2016) available from their website at <http://marine.copernicus.eu/services-portfolio/access-to-products/>. Daily data of salinity and mixed layer depth from the same source was used for the buoyancy flux and convective velocity scale ( $w$ ) calculations (see Section 3.3).

Datasets were averaged from its original temporal resolution to monthly values. The spatial grid was defined to cover the area between  $52^\circ - 66^\circ\text{N}$  and  $10^\circ - 32^\circ\text{E}$  with a spatial resolution of  $1/24^\circ$  in latitude and longitude (equivalent to a  $4 \times 4$  km grid at the equator). Variables were interpolated – when necessary – using a bilinear interpolation method to match the specified spatial grid.

### 3.3. Air–sea flux calculations

FluxEngine is an open source software for air–sea gas flux calculations available via <http://github.com/oceanflux-ghg/FluxEngine>. FluxEngine was developed with the aim of providing a standardized toolbox for robust flux calculation that allows the incorporation of a variety of data sources (i.e. Earth observation, model, and *in situ* data). The toolbox also provides flexibility in terms of available methodologies and transfer velocity parametrizations. A detailed description of the FluxEngine toolbox can be found in Shutler et al. (2016) and Holding et al. (2019).

In this study, we used the FluxEngine toolbox to calculate air–sea  $\text{CO}_2$  fluxes for six different scenarios using the rapid model approach (Eq. (2)). Concentrations of  $\text{CO}_2$  ( $\text{g m}^{-3}$ ) in the atmosphere and in seawater were calculated from the input data (i.e. from atmospheric  $\text{CO}_2$  dry mole fractions and  $p\text{CO}_2$  in seawater, respectively). We used the same input fields (Section 3.2) for each of the six different scenarios, but different parametrizations of the gas transfer velocity were used in each case. A summary of the gas transfer velocity equations is shown in Table 1. A detailed description of each parametrization follows in the text (for the corresponding references see Table 1).

The base-case scenario considers the wind-based parametrization of the transfer velocity suggested by Nightingale et al. (2000) (hereafter

**Table 1**

Summary of the gas transfer velocity parametrizations used in this study.

| Name             | Equations   | References   |
|------------------|---|--|
| N00 <sup>a</sup> | $k_u$ (Eq. (9))   | Nightingale et al. (2000)                            |
| (a) N00+conv     | $k = k_u + k_c$ ;<br>$k_c = 3022w - 20$                                   | Rutgersson and Smedman (2010)                        |
| (b) N00+rain     | $k = k_u + (1 - \exp^{-\alpha\beta})k_r$ ;<br>$k_r = 63.02KEF_r^{0.6242}$ | Harrison et al. (2012), Ashton et al. (2016)         |
| (c) N00+surf     | $k = k_u R$ ;<br>$R = 1 - (0.0046T_{skin})^{2.5673}$                      | Pereira et al. (2018)                                |
| (d) N00+all      | $k = (k_u + k_c + k_r)R$  | –  |
| (e) RS10         | $k = k'_u + k_c$ ;<br>$k'_u = 0.24U_{10}^2$ ;<br>$k_c = 3022w - 20$       | Rutgersson and Smedman (2010), Norman et al. (2013a) |

<sup>a</sup>Base-case scenario.

referred to as N00) obtained from dual tracer measurements in the North Sea,

$$k_u = (0.222U_{10}^2 + 0.333U_{10})\sqrt{600/Sc}, \quad (9)$$

In addition to the base-case scenario, we used four different parametrizations that include additive terms to the N00 gas transfer velocity. The additive terms were: (a) water-side convection, in such way that  $k = k_u + k_c$ , where  $k_c = 3022w - 20$  is the transfer velocity term associated to ocean convection, and  $w = (Bz_{ml})^{1/3}$  is the convective velocity scale where  $B$  is the buoyancy flux defined according to Jeffery et al. (2007) and  $z_{ml}$  is the mixed-layer depth; (b) a non-linear term accounting for the effect of precipitation in such way that  $k = k_u + (1 - \exp^{-\alpha\beta})k_r$ , with  $\alpha = 0.3677$ ,  $\beta = KEF_r/KEF_w$  where  $KEF_r = 0.0112R_n$  and  $KEF_w = \rho_a u_*^3$  represent the rain- and wind-induced kinetic energy flux, respectively,  $R_n$  is the precipitation rate,  $\rho_a$  is the density of air,  $u_*$  is the friction velocity, and the rain-induced gas transfer velocity is given by  $k_r = 63.02RE F_r^{0.6242}$ ; (c) biological surfactant suppression term given by  $R = 1 - (0.0046T_{skin})^{2.5673}$  as a function of the skin temperature ( $T_{skin}$ ), such that  $k = k_u R$ ; and d) a case including all the parameters from (a) to (c), i.e., water-side convection, precipitation, and surfactant suppression. Finally, we included a last case with  $k = k'_u + k_c$  where  $k'_u = 0.24U_{10}^2$  was obtained as the fit of transfer velocity data calculated in the Baltic Sea from eddy covariance fluxes, and  $k_c$  is the same as in case (a).

Net integrated fluxes over the Baltic Sea and the individual sub-regions (GB, GF, CB, and SB) were calculated from the monthly mean fluxes at each grid cell. The net fluxes were integrated over each specific region, therefore, information about the area of the pixel, the ice coverage, and the land/sea proportion were required. The area of each grid cell was calculated based on the original spatial resolution of the grid ( $1/24^\circ$ ) in latitude and longitude assuming an ellipsoidal Earth. Ice coverage was taken into account following a linear relationship from 10% to 90%, where the net flux of each grid cell was reduced by the corresponding ice-cover value (Takahashi et al., 2009). Ice coverage below 10% was considered to have a negligible effect on the flux, while values above 90% were set to the maximum value of 90% to account for leads, polynyas, etc. The land mask specifying the proportion of land in each grid cell, as well as the sea masks defining each region (i.e. the entire Baltic Sea or the individual sub-regions), were obtained from a high-resolution ( $\sim 1$  nm) topography of the Baltic Sea (Seifert et al., 2001). The integrated net flux tool used for the calculations is part of the FluxEngine and a detailed description can be found in Shutler et al. (2016).

## 4. Results

### 4.1. General conditions in the baltic sea

The wind speed showed a seasonal behaviour with high values during winter and milder conditions during summer (Fig. 2a). This



seasonality was observed during the three years analysed in the study. Nevertheless, differences in the monthly means among the years were relevant for the net air–sea CO<sub>2</sub> fluxes. Lower monthly wind speeds were observed from January to September in 2010 compared to the other two years; 2009 showed the highest monthly means during the summer months, and 2011 presented some high monthly means during the winter months.

The ocean skin temperature (Fig. 2b) presented a clear seasonal variability with low values during winter and high temperatures during summer. Positive air–sea temperature gradients (Fig. 2c) from August to February indicate cooling of the surface. On the contrary, from March to July, the negative gradient suggests a warming of the sea surface. Following the temperature gradients, the oceanic mixed layer depth showed higher values during the winter months when larger heat losses occurred. Shallow mixed layer depths were observed during the summer (Fig. 2d). Slightly larger monthly precipitation rates were observed during the summer months (Fig. 2e).

The CO<sub>2</sub> concentration gradients (Fig. 2g) were – to a great extent – modulated by changes in the seawater CO<sub>2</sub> concentrations throughout the year, while atmospheric concentrations showed smaller seasonal variability (Fig. 2f). The seasonal variability of the sea surface water concentrations in the Baltic Sea is associated to biological activity (Thomas and Schneider, 1999; Schneider et al., 2003), with high consumption rates of CO<sub>2</sub> during spring and summer leading to the observed negative values of  $\Delta C$ . From September to March, positive values of  $\Delta C$  were observed due to increased seawater CO<sub>2</sub> concentrations. High values of CO<sub>2</sub> concentration in the upper ocean are usually associated with a decrease in the productivity during the winter months and to the transport of CO<sub>2</sub>-enriched water masses to the surface due to deep layer mixing. The annual cycle of  $\Delta C$  presented a similar behaviour during 2009 and 2010. During 2011, stronger gradients occurred at the beginning of the year, but lower positive values at the end of the year compared to 2009 and 2010.

#### 4.2. Gas transfer velocity

The annual cycle of the gas transfer velocities (Fig. 3) was – to great extent – modulated by the behaviour of the wind. Higher values of the gas transfer velocity (here expressed as  $k_{660}$ ) were observed during winter and associated to higher wind speeds. The lowest  $k_{660}$  values observed during spring can be linked to the lowest wind speeds (see Fig. 2a). However, the impact of the different driving mechanisms (i.e. water-side convection, precipitation, and surfactants) also affected the seasonality of the gas transfer velocity. Convective processes were particularly relevant during winter when the cooling of the surface induced vertical convective mixing. Cases including convective processes (N00+conv, N00+all, and RS10) showed higher transfer velocity values, thus, promoting an increase of the upward flux during the winter months. The highest values of the gas transfer velocity were observed in December reaching up to 30.6 cm h<sup>-1</sup> for the three cases including convection. Surfactants had an effect mostly during the summer, when surface water temperatures were high (see Fig. 2b). The effect of precipitation was barely perceivable throughout the year (i.e. the blue line from N00+rain is over the black line from N00 in Fig. 3).

For comparative purposes, the results of the six gas transfer velocity formulations used in this study were also compared to some commonly-used wind-based parametrizations ( $k_w$ ). The wind-based parametrizations, including the base-case from Nightingale et al. (2000) (N00), and parametrizations by Ho et al. (2006), McGillis et al. (2001), and Wanninkhof (2014) are represented by the shaded area in Fig. 3 (see Appendix B for details about the wind-based formulations).

The behaviour of the gas transfer velocity in the different sub-regions of the Baltic Sea showed a significant spatial variability (Fig. 4). The results of the gas transfer velocity in each sub-region were compared to the average transfer velocity in the Baltic Sea (grey dashed

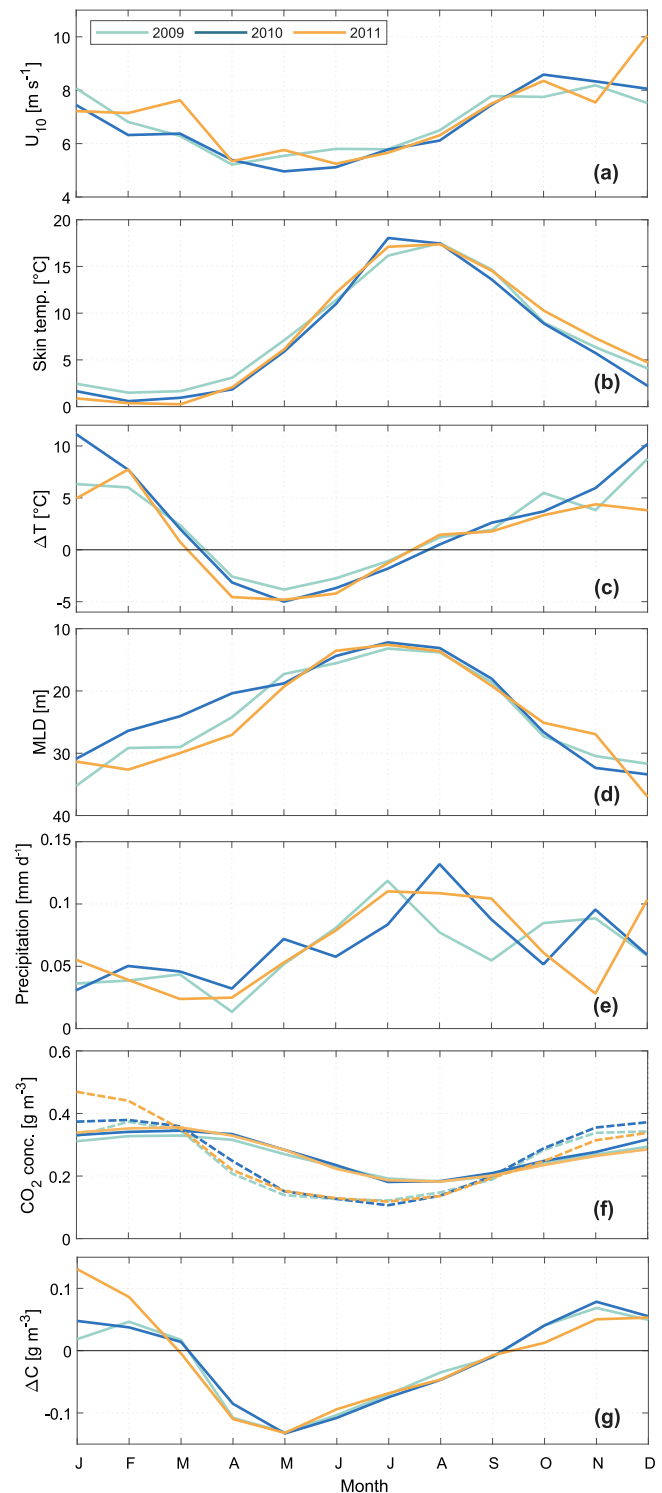


Fig. 2. Monthly means of (a) wind speed, (b) surface skin temperature, (c) air–sea temperature gradient, (d) mixed layer depth, (e) mean precipitation rate, (f) CO<sub>2</sub> concentrations in the atmosphere (solid lines) and in the seawater (dashed lines), and (g) CO<sub>2</sub> concentration gradient ( $\Delta C$ ). The lines represent the different years: 2009 (light blue), 2010 (dark blue), and 2011 (yellow).

line and shaded area in Fig. 4) to assess the relative impact of taking into account the different driving mechanisms in each region.

In the Gulf of Bothnia, large values of the gas transfer velocity occurred throughout the year in comparison to the mean values of the Baltic Sea. This was particularly noticeable during winter when

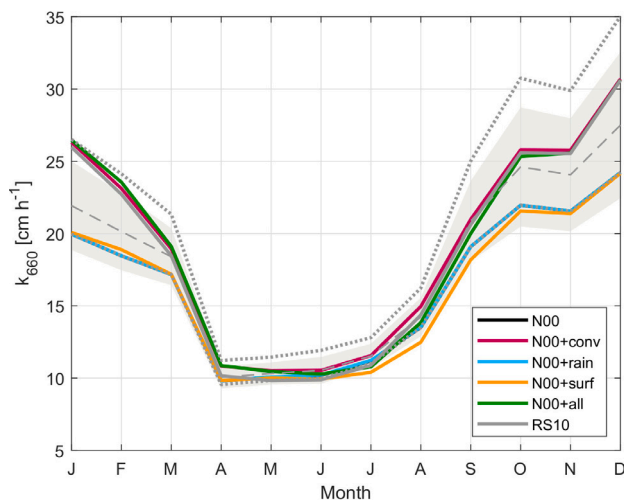


Fig. 3. Monthly means of the gas transfer velocity ( $k_{660}$ ) in the Baltic Sea using six different parametrizations as described in Table 1. The grey dashed line represents the mean gas transfer velocity from a set of commonly-used wind-based parametrizations (see Table B.5), the shaded area is the standard deviation, and the dotted lines are the minimum and maximum values.

the highest values of  $k_{660}$  (up to  $32.3 \text{ cm h}^{-1}$ ) were observed for the cases when convective processes were included. During summer, in the Gulf of Bothnia all the parametrizations showed higher values than the mean, including the base-case scenario. In the Gulf of Finland, the cases including convective processes were close to the Baltic Sea average values during this period. The rest of the cases fell below the average with the minimum values corresponding to the case including surfactants. Due to its surface extent, the Central Basin was the major contributor to the overall behaviour of the Baltic Sea. For this region, the largest values of  $k_{660}$  were observed during winter for cases including convection, while the rest of the cases remained fairly low throughout the year. Finally, the transfer velocity in the Southern Basin presented a similar pattern than in the Gulf of Finland, with noticeable low values for the N00, N00+rain and N00+surf cases.

#### 4.3. Air-sea $\text{CO}_2$ fluxes

Air-sea  $\text{CO}_2$  fluxes were calculated using six different transfer velocity parametrizations (Table 1) over a three-year period from 2009 to 2011. The average annual cycle of the six different flux estimates (Fig. 5a) showed that the Baltic Sea was a source of atmospheric  $\text{CO}_2$  (positive flux) during the winter months (October to February) and a sink (negative flux) during the summer (April to August). This behaviour is consistent with the patterns observed in the sea surface concentrations (Fig. 2f), and with the derived  $\text{CO}_2$  concentration gradients,  $\Delta C$  (Fig. 2g).

The differences in the calculated  $\text{CO}_2$  fluxes using the different parametrizations were largest during the winter months mostly due to convective processes enhancing the upward transport (Figs. 5b). During summer, convection and surfactants seemed to act as competing mechanisms controlling the flux. Convective processes slightly enhanced the downward flux, while surfactants tended to suppress it. Precipitation seemed to have little effect on the air-sea fluxes year-round.

At sub-regional scale, the effect of including additional parameters in the flux calculation (i.e. using N00+all) was particularly relevant during the winter months. The air-sea  $\text{CO}_2$  fluxes in the four sub-regions of the Baltic Sea were larger from October to February when the N00+all formulation was used, in comparison to the fluxes obtained using solely the wind-based transfer velocity N00 (Fig. 6). On average, an increase in the flux of 22% was observed in the Gulf Bothnia, 17% in the Gulf of Finland, 22% in the Central Basin, and 36% in the Southern Basin. Using N00+all parametrization had a negligible effect on the air-sea  $\text{CO}_2$  fluxes during the summer.

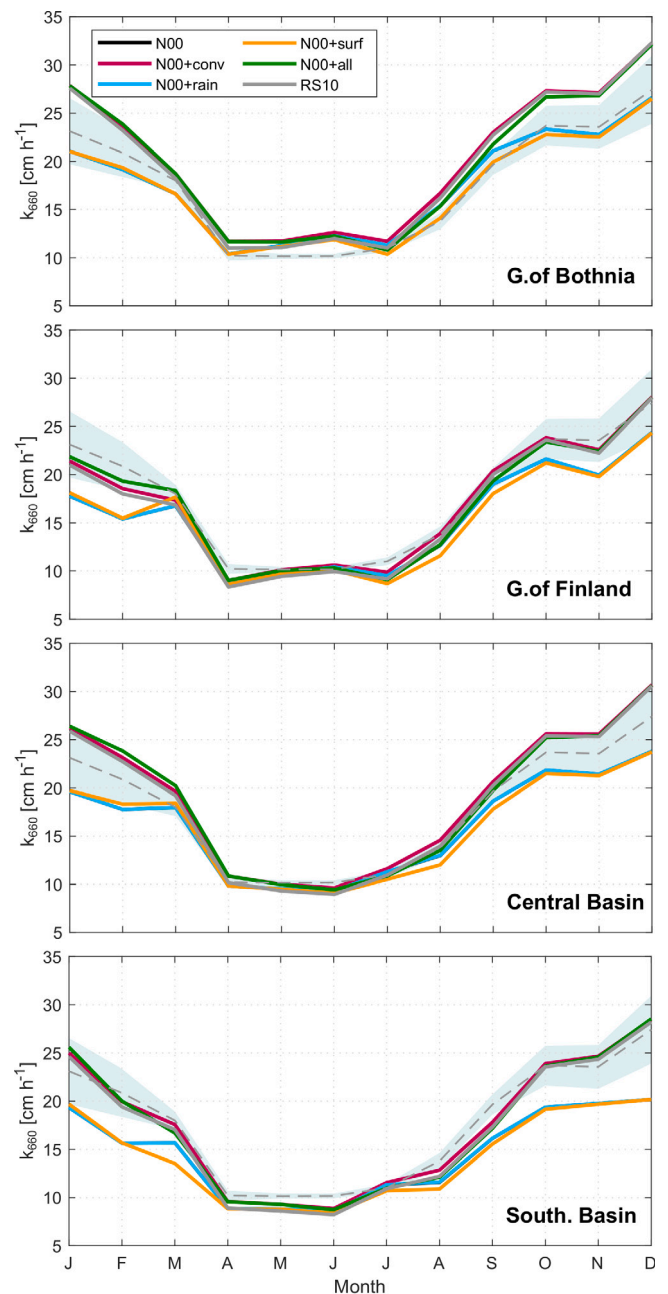


Fig. 4. Annual cycle of gas transfer velocity ( $k_{660}$ ) using six different parametrizations (Table 1) in the four sub-regions of the Baltic Sea. The grey dashed line represents the mean gas transfer velocity of the entire Baltic Sea, and the shaded area is the standard deviation.

#### 4.4. Net integrated $\text{CO}_2$ fluxes

The annual net integrated fluxes in the Baltic Sea ranged between 0.0 and  $-0.88 \text{ TgC y}^{-1}$  among the different cases, suggesting that – on average – the Baltic Sea was a net sink of  $\text{CO}_2$  during the study period (grey bars in Fig. 7a). Including water-side convection on the air-sea  $\text{CO}_2$  calculations resulted in a decrease of 72% in the net uptake in comparison to the base-case, i.e. from  $-0.85 \text{ TgC y}^{-1}$  corresponding to the N00 case to  $-0.24 \text{ TgC y}^{-1}$  when N00+conv was used. In a similar way, using N00+all and RS10 resulted in a decrease of the net  $\text{CO}_2$  flux mostly due to impact of convection (75% and 100%, respectively). For these cases, the decrease in the uptake was caused by the large upward fluxes during the winter months. Surfactants

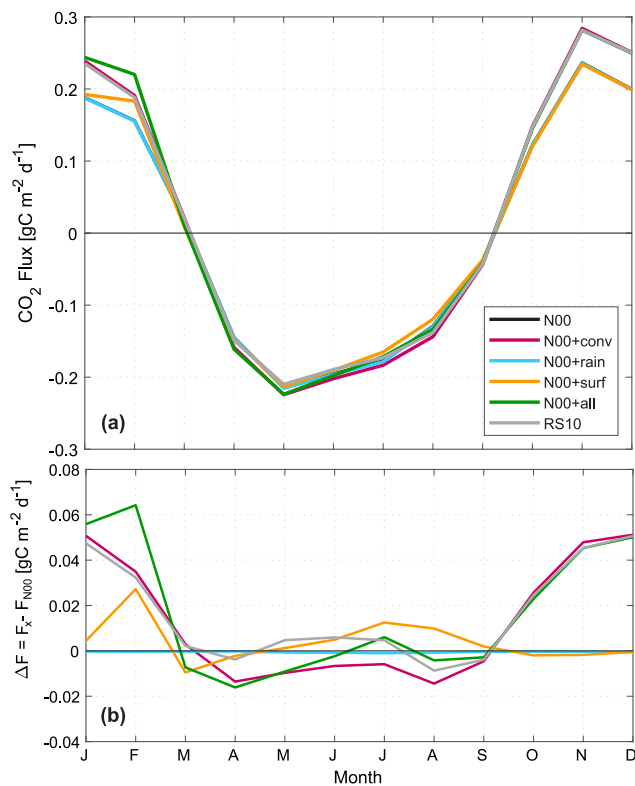


Fig. 5. Average annual cycle of (a) air-sea CO<sub>2</sub> fluxes calculated using the six gas transfer velocity parametrizations described in Table 1, (b) air-sea CO<sub>2</sub> flux from each gas transfer velocity parametrization relative to the base-case scenario ( $\Delta F = F_x - F_{N00}$ ).

caused a reduction of 7% in the annual net flux. Precipitation, on the contrary, was the only parameter which resulted in an overall increase (4%) of the downward fluxes. Therefore, larger negative net CO<sub>2</sub> flux was observed when N00+rain was used, reaching the value of  $-0.88 \text{ TgC y}^{-1}$ . The differences in the net flux for each case relative to the base-case scenario are shown in Fig. 7a and Table A.2.

In terms of the inter-annual variability, we observed larger net CO<sub>2</sub> uptake during 2009 than in 2010 and 2011 (Fig. 7b). Higher wind speeds during the summer of 2009 (Fig. 2a) caused larger downward fluxes, hence, a larger CO<sub>2</sub> uptake. For the base-case scenario, the three years presented negative net CO<sub>2</sub> fluxes. However, positive net fluxes were observed during 2010 for the cases where water-side convection was taken into account. Larger air-sea temperature gradients during winter (Fig. 2c) and lower wind speeds (Fig. 2a) suggest a strong impact of the convective processes during 2010. Moderate negative net fluxes were observed during 2011 for all cases, despite the large  $\Delta C$  and high wind speeds (Fig. 2a, g). The effect of including precipitation and surfactants into the gas transfer velocity parametrizations, seemed to be less significant for the inter-annual variability than convective processes.

The average net CO<sub>2</sub> fluxes indicated that the four sub-regions of the Baltic Sea tended to be net sinks of CO<sub>2</sub> (Fig. 8a). However, the effect of the precipitation, surfactants, and water-side convection on the net CO<sub>2</sub> fluxes showed a spatial distribution associated with the individual characteristics of each sub-region. The largest fluxes, as well as the largest differences relative to the base case scenario, were observed in the Central Basin—the largest basin. The Gulf of Finland showed the smallest fluxes. Water-side convection was the parameter having the greatest effect on the fluxes in all sub-regions, except for the Gulf of Finland where negligible differences were observed when using the different gas transfer velocity parametrizations (Fig. 8b). The net flux differences between each case and the base-case scenario are shown in

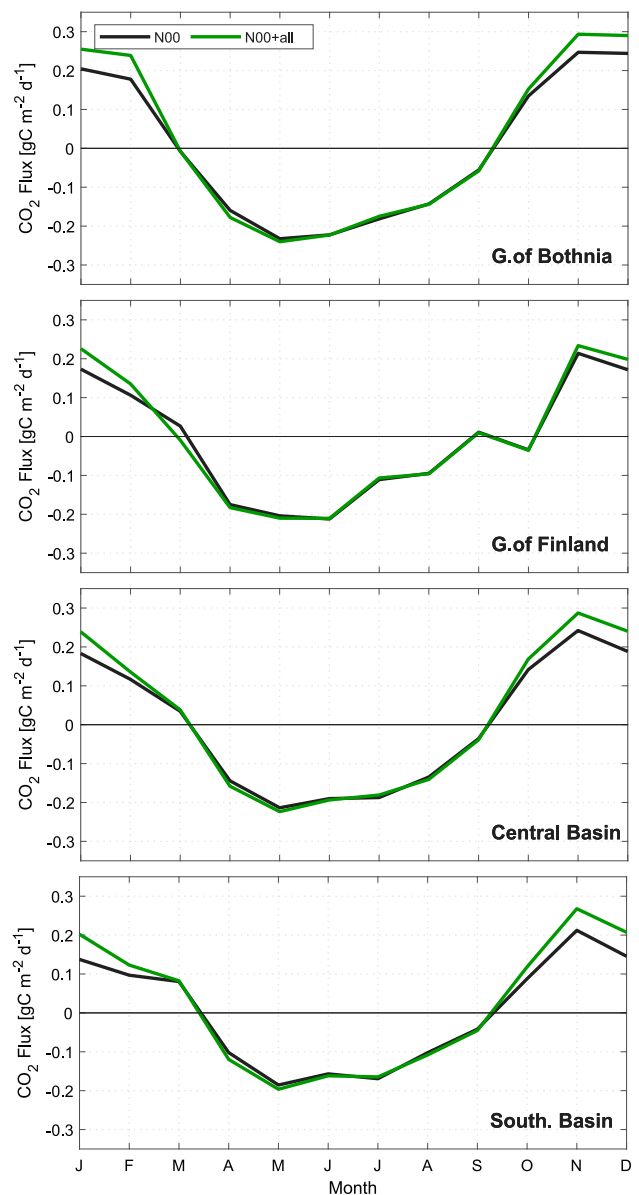
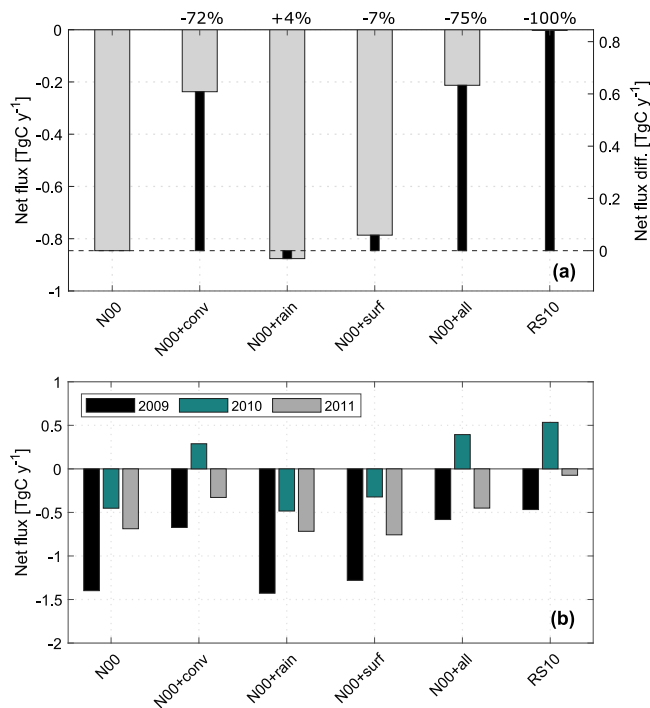


Fig. 6. Annual cycle of air-sea CO<sub>2</sub> fluxes in the four sub-regions of the Baltic Sea using two different transfer velocity parametrizations. The black line represents the fluxes using the wind-based parametrization (N00); the green line represents the fluxes using the parametrization including wind, precipitation, surfactants and water-side convection (N00+all).

Fig. 8b, while a summary of the relative difference (%) of the net flux can be found in Table A.3.

The air-sea CO<sub>2</sub> flux estimations showed that the fluxes in the coastal regions (Fig. 1b), here defined as regions with depths smaller than 20 m, were larger than in the open sea (Fig. 9a). The largest fluxes were observed when precipitation (N00+rain) was taken into account, both in the coast and the open sea. In terms of the seasonal cycle (not shown), the air-sea CO<sub>2</sub> exchange in the coast was lower than in the open sea during the winter. In summer the opposite was true, with larger fluxes in the coastal region than in the open sea.

From the net fluxes in Fig. 9b, it is clear that the main contribution to the total budget was associated to the open sea due to its larger surface extent. This is true for the base-case scenario (N00) and cases when convective processes were not taken into account. For the cases where convection was considered, a significant reduction of the open sea contribution was observed (e.g. 81% reduction when N00+conv is



**Fig. 7.** (a) Average net flux of CO<sub>2</sub> in the Baltic Sea (grey bars, primary axes), and net CO<sub>2</sub> flux difference for each case relative to the base-case scenario (black bars, second axes) calculated as  $\Delta F_{net} = F_{net_x} - F_{net_{N00}}$ . Results from 2009, 2010 and 2011 were included in the average. The numbers represent the percentage of relative difference of the net flux ( $\Delta F_{net}/F_{net_{N00}} \times 100$ ). (b) Annual net flux in the Baltic Sea during 2009, 2010, and 2011. For (a) and (b) the fluxes were calculated using each of the gas transfer velocity parametrizations described in Table 1.

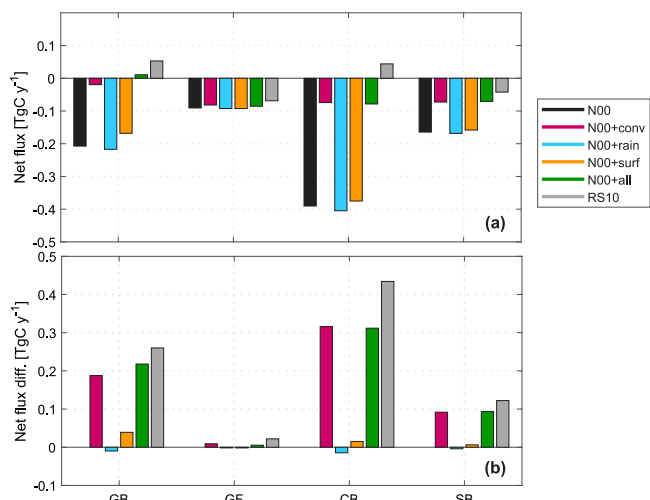


**Fig. 8.** (a) Net flux of CO<sub>2</sub> in the four sub-regions of the Baltic Sea: Gulf of Bothnia (GB), Gulf of Finland (GF), Central Basin (CB), and Southern Basin (SB). (b) Net CO<sub>2</sub> flux difference for each case relative to the base-case scenario (N00). The colours represent each of the six transfer velocity parametrizations described in Table 1.

used). Even though convective processes also had an effect in coastal regions (e.g. 38% with N00+conv), the impact was considerably smaller than that in open sea. Surfactants resulted in a 6% and 7% suppression in coastal regions and open sea, respectively. Whereas precipitation represented an enhancement of 3% in coastal regions and 4% in open sea. Table A.4 summarizes the relative difference of net fluxes in the coastal zone and open sea for the different formulations.

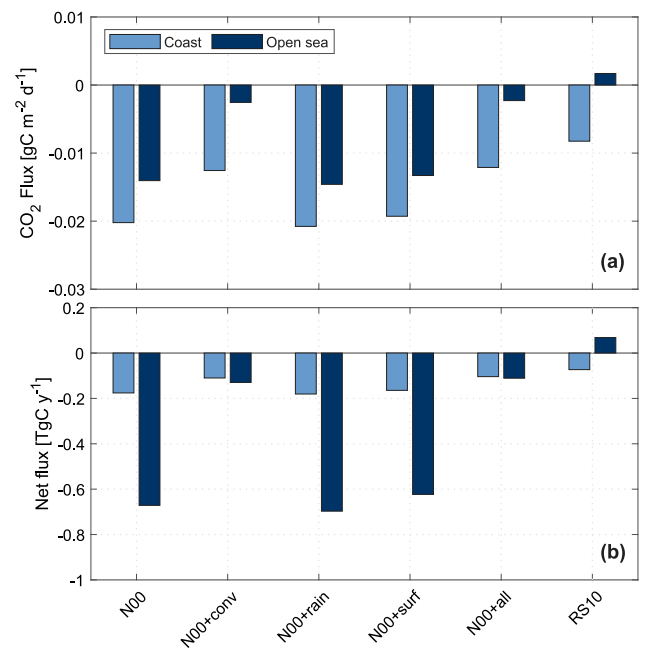


**Fig. 9.** Coastal and open sea (a) air-sea CO<sub>2</sub> fluxes and (b) net integrated air-sea CO<sub>2</sub> fluxes. The fluxes were calculated using each of the gas transfer velocity parametrizations described in Table 1.

## 5. Discussion

In this study, we evaluated the effect of including parametrizations of some relevant processes on air-sea CO<sub>2</sub> exchange for the Baltic Sea and its sub-regions. The results showed that the spatial and temporal variability in the air-sea CO<sub>2</sub> flux was partly caused by forcing mechanisms other than wind speed. With the results presented here, we highlight the importance of including relevant parameters on the gas transfer velocity parametrization and provide a better understanding of the temporal and spatial variability of CO<sub>2</sub> fluxes in the region. In the Baltic Sea, the average wind speed in the fall-winter period is higher than in spring-summer; surfactant concentrations are particularly high during the summer cyanobacterial bloom period under warmer sea surface temperature conditions; water-side convection is particularly relevant during winter when sea surface heat losses drive strong vertical mixing; and changes in the amount and type of precipitation throughout the year have different effects on the air-sea CO<sub>2</sub> fluxes. Accounting for such variability is essential to constrain the local and regional CO<sub>2</sub> flux estimates through adequate gas transfer velocity parameterizations. The issue about whether the Baltic Sea is a sink or a source of CO<sub>2</sub> is still a matter of debate and is beyond the scope of this study.

The seasonal variability was affected by convective processes, precipitation, and surfactants at regional and sub-regional scales (Figs. 5 and 6). Based on the results of the integrated net fluxes, we showed that the inter-annual variability was also affected by the forcing mechanisms evaluated here, particularly by water-side convection (Fig. 7b). The net CO<sub>2</sub> fluxes using the six formulations showed the sensitivity of the budget calculations in the region (Fig. 7a). Even though the total contributions were rather small (less than 1 TgC y<sup>-1</sup>) – and we do not intend to establish absolute numbers for the net flux – the choice of the transfer velocity formulation was shown to have a strong effect on the total budget, in some cases even changing the average behaviour of the region from being a sink to become a source of CO<sub>2</sub>.

Convective processes were found to be important both at regional and sub-regional scales. Inter-annual (Fig. 7b) and spatial (Fig. 8) variabilities were mostly affected by convection rather than by other



processes. The importance of water-side convection in the Baltic Sea has been highlighted in previous studies (Rutgersson and Smedman, 2010; Rutgersson et al., 2011). Norman et al. (2013b) found a maximum impact of 20% when including water-side convection on the gas transfer velocity parametrization. In this study, the impact of water-side convection on the air–sea fluxes was reflected as an increase of the upward fluxes during winter. We found that convection can have a relative impact of up to 28% in the monthly fluxes during winter time (see Fig. 5). Such impact represents a reduction of 72% to the average uptake of the Baltic Sea relative to the base-case scenario, and between 10% and 90% in the different sub-regions being the Gulf of Bothnia the most affected region Appendix A. Open sea areas were also highly affected by convective processes (Fig. 9 and Table A.4).

The effect of surfactants was perceived by the low values of  $k_{660}$  from June to November which resulted in the restriction of the (downward) fluxes during the summer months and – to a lesser extent – in the (upward) fluxes towards the end of the year (Fig. 5). The overall effect of surfactants was noticeable as a reduction of the downward fluxes during summer in the entire Baltic Sea (7%) and in the different sub-regions (ranging between 4% and 19%). Pereira et al. (2018) found a reduction of 0.3–6.5% in the gas transfer velocity in three coastal locations based on the % suppression-SST relationship (corresponding to the parametrization used in this study), and 2%–24% in the Atlantic Ocean compared to values of 2%–32% from measurements.

Precipitation was the only parameter that resulted in an enhancement of the downward fluxes in the Baltic Sea, this contribution represented an increase of 4% in the net uptake relative to the base case. Using the same gas transfer velocity formulation, Ashton et al. (2016) found that – at a global scale – the effect of rain can lead to an increase of the ocean uptake of 6%. Changes in the net air–sea CO<sub>2</sub> flux due to precipitation at regional scale were estimated, in the same study, to be between 2.4% and 15%, in all cases increasing the ocean sink.

Four key aspects must be considered when addressing the results of this research: (1) the suitability of the gas transfer velocity parametrizations for the Baltic Sea conditions, (2) the monthly resolution of the input data and air–sea flux calculations, (3) the suitability of the pCO<sub>2</sub> input data, and (4) the uncertainties associated to the flux calculations. These aspects – briefly discussed in the following paragraphs – also hindered the possibility of addressing the absolute numbers of the air–sea CO<sub>2</sub> budgets.

As discussed in the previous paragraphs, the results found in this study are in good agreement with other studies using the same parametrizations (Norman et al., 2013b; Pereira et al., 2018; Ashton et al., 2016). However, most of the parametrizations used in this study were not developed for marginal seas, and they are rarely based on datasets including a good representation of the coastal regions. The exception is the parametrization developed by Rutgersson and Smedman (2010) (i.e. RS10), where the terms including the forcing of the wind and the effect of water-side convection were both derived from data obtained at a coastal station in the Baltic Sea. For the cases including precipitation and surfactant suppression, the limitations of using parametrizations that might poorly represent the Baltic Sea conditions must be considered. On the one hand, we assumed that the precipitation data only characterizes rainfall, while other types of precipitation – such as snow, ice, and sleet – are most certainly relevant for the Baltic Sea. On the other hand, surfactant suppression might be relevant in areas of the Baltic Sea with high input of organic matter from land, as well as during summer, when strong cyanobacterial blooms occur in the region. Sea surface temperature appears to be a robust proxy for surfactant activity (Pereira et al., 2018), however, it does not fully account for the spatio-temporal variability of surfactant control on air–sea gas exchange. The N00+surf parametrization is solely temperature dependent, and does not include other non-linear effects associated to biological processes. Therefore, it might not account for the total effect and variability of surfactants in the Baltic Sea.

The monthly resolution of the input data and the derived flux estimates entails an additional limitation. Particularly in coastal areas, where the high variability of the physical and biogeochemical processes might not be fully represented by the monthly averages. However, the air–sea CO<sub>2</sub> fluxes in the open sea are also constrained by these limitations. Using monthly averages of precipitation rate, for example, has significant drawbacks that must be taken into account (see Ashton et al., 2016). Such limitations come from the impossibility to capture intense episodic or extreme events. The overall effect of these events on the air–sea CO<sub>2</sub> fluxes at global and regional scales is still an area of investigation. In Parard et al. (2016), the effect of using monthly input data to account for biological activity in the pCO<sub>2</sub> estimations is discussed.

A recent study by Watson et al. (2020), pointed out the importance of using adequate surface CO<sub>2</sub> concentration data for accurate air–sea CO<sub>2</sub> flux calculations. According to the study, the sea surface in-situ pCO<sub>2</sub> data must be corrected for temperature gradients between the surface and the measurement depth, and for the effect of the cool ocean surface skin before calculating the air–sea CO<sub>2</sub> flux. In this study, the effect of the cool skin temperature, discussed by Watson et al. (2020), is accounted for following Donlon et al. (2002) (See Section 3.2). However, the correction of the in-situ observations taken at a few metres depth, and used for the generation the pCO<sub>2</sub> fields entails a much complicated issue not addressed here.

Finally, the sensitivity analysis presented here is not dependent on the sources or the accuracy of the input variables. The analysis of absolute fluxes, however, would require an in-depth uncertainty analysis. The uncertainties associated to the air–sea CO<sub>2</sub> flux come from the uncertainties of each individual term involved in the flux calculation (i.e. uncertainties associated to the input data and uncertainties associated to the gas transfer velocity parametrizations). Such analysis is beyond the scope of this study.

## 6. Conclusions

In this study, we present – with a sensitivity analysis – the impact of water-side convection, precipitation, and surfactants on air–sea gas exchange in the Baltic Sea. We showed that the inter-annual and spatial variability of the fluxes was not solely modulated by the wind speed, but also by these processes. The gas transfer velocity formulations used in this study were selected based on the library functions within the FluxEngine toolbox and the available input data. We do not consider these – or any other formulations – to be more or less adequate for air–sea flux calculations in the Baltic Sea. Moreover, the aim of this study is not to present accurate quantification of the fluxes but to show the importance of accounting for relevant processes in the air–sea gas exchange calculations in marginal seas. We are aware that other processes not considered in this study may also be relevant (wave-field, ice edges, etc.), and we therefore encourage further investigation of the relevant processes on air–sea gas exchange. The Baltic Sea provides a unique test field for such investigations with its large biogeochemical gradients, different wave characteristics and limited-fetch areas, large concentrations of land-derived organic material, and partial ice coverage.

## Acknowledgements

The authors would like to thank John Prytherch for the valuable comments on the manuscript. This work was performed within the project BONUS INTEGRAL, which receives funding from BONUS (Art 185), funded jointly by the EU, the German Federal Ministry of Education and Research, the Swedish Research Council Formas, the Academy of Finland, the Polish National Centre for Research and Development, and the Estonian Research Council, Estonia.

**Table A.2**

Relative difference between the air–sea CO<sub>2</sub> net flux in the Baltic Sea from the different gas transfer velocity parametrizations including water-side convection, precipitation, and surfactant suppression, and the base-case scenario (N00).

| Reference <sup>a</sup> | N00+conv | N00+rain | N00+surf | N00+all | RS10  |
|------------------------|----------|----------|----------|---------|-------|
| -0.85                  | -72%     | +4%      | -7%      | -75%    | -100% |

<sup>a</sup>Net CO<sub>2</sub> fluxes (TgC y<sup>-1</sup>) using N00 formulation.

**Table A.3**

Same as Table A.2, in this case including data corresponding to the Baltic Sea sub-regions.

| Name                   | G. of Bothnia | G. of Finland | Central Basin | South. Basin |
|------------------------|---------------|---------------|---------------|--------------|
| Reference <sup>a</sup> | -0.21         | -0.09         | -0.39         | -0.17        |
| N00+conv               | -91%          | -10%          | -81%          | -56%         |
| N00+rain               | +5%           | +2%           | +2%           | +2%          |
| N00+surf               | -19%          | +2%           | -4%           | -4%          |
| N00+all                | -105%         | -6%           | -80%          | -57%         |
| RS10                   | -126%         | -24%          | -111%         | -74%         |

<sup>a</sup>Net CO<sub>2</sub> fluxes (TgC y<sup>-1</sup>) using N00 formulation.

**Table A.4**

Same as Table A.2, in this case including data corresponding to the coastal and open sea regions.

| Name                   | Coastal zone | Open sea |
|------------------------|--------------|----------|
| Reference <sup>a</sup> | -0.18        | -0.67    |
| N00+conv               | -38%         | -81%     |
| N00+rain               | +3%          | +4%      |
| N00+surf               | -6%          | -7%      |
| N00+all                | -41%         | -84%     |
| RS10                   | -58%         | -110%    |

<sup>a</sup>Net CO<sub>2</sub> fluxes (TgC y<sup>-1</sup>) using N00 formulation.

**Table B.5**

Summary of equations and references of wind-based transfer velocity ( $k_u$ ) parametrizations.

| Name  | Description                 | References                |
|-------|-----------------------------|---------------------------|
| N00   | $k_u$ from Eq. (9)          | Nightingale et al. (2000) |
| H06   | $k_u = 0.266U_{10}^2$       | Ho et al. (2006)          |
| McG01 | $k_u = 3.3 + 0.026U_{10}^3$ | McGillis et al. (2001)    |
| W14   | $k_u = 0.251U_{10}^2$       | Wanninkhof (2014)         |

**Appendix A. Relative impact of the driving mechanisms on air–sea fluxes**

The relative difference between the net integrated fluxes from the different gas transfer velocity parametrizations (Table 1) and the base-case scenario (N00) is shown in Table A.2. Note that the relative differences calculated for the air–sea CO<sub>2</sub> flux and for the net integrated fluxes are virtually the same. Therefore, only the those corresponding to the net integrated CO<sub>2</sub> fluxes are presented here.

Table A.3 summarizes the relative difference of net fluxes for the Baltic Sea sub-regions relative to the base-case scenario. Similarly, Table A.4 shows the relative difference for the net integrated CO<sub>2</sub> fluxes in the coastal zone and the open sea.

**Appendix B. Wind-based parametrizations**

Wind-based gas transfer velocity ( $k_u$ ) parametrizations were used for comparative purposes. A summary of the equations used in this study and the corresponding references is presented in Table B.5. The annual cycle of  $k_u$  is shown in Fig. B.10.

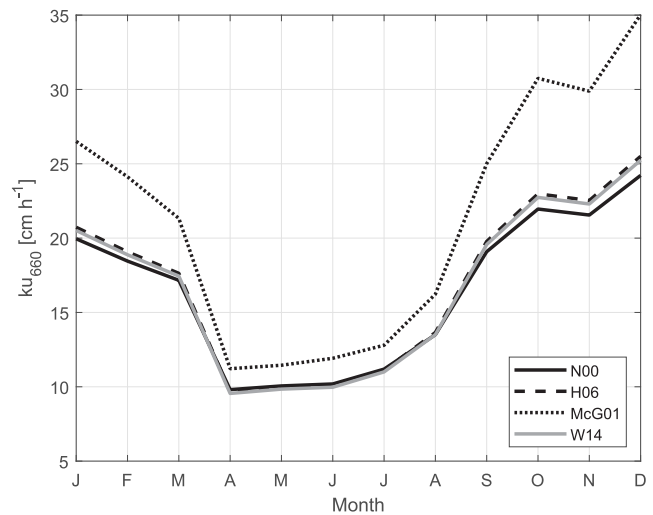


**Fig. B.10.** Wind-based gas transfer velocity parametrizations.

**References**

Ashton, I.G., Shutler, J.D., Land, P.E., Woolf, D.K., Quartly, G.D., 2016. A sensitivity analysis of the impact of rain on regional and global sea–air fluxes of CO<sub>2</sub>. *PLoS One* 11 (9).

Bergström, S., Carlsson, B., 1994. River runoff to the Baltic Sea:1950–1990. *Ambio* 23 (4–5), 280–287.

Borges, A.V., Delille, B., Frankignoulle, M., 2005. Budgeting sinks and sources of CO<sub>2</sub> in the coastal ocean: Diversity of ecosystems count. *Geophys. Res. Lett.* 32, L14601.

Cai, W.-J., Dai, M., Wang, Y., 2006. Air–sea exchange of carbon dioxide in ocean margins: A province-based synthesis. *Geophys. Res. Lett.* 33 (12).

Chen, C.-T.A., Liu, K.-K., Macdonald, R., 2003. Continental margin exchanges. In: *Ocean Biogeochemistry*. Springer, pp. 53–97.

Donlon, C.J., Martin, M., Stark, J., Roberts-Jones, J., Fiedler, E., Wimmer, W., 2012. The operational sea surface temperature and sea ice analysis (OSTIA) system. *Remote Sens. Environ.* 116, 140–158.

Donlon, C., Minnett, P., Gentemann, C., Nightingale, T., Barton, I., Ward, B., Murray, M., 2002. Toward improved validation of satellite sea surface skin temperature measurements for climate research. *J. Clim.* 15 (4), 353–369.

Esters, L., Landwehr, S., Sutherland, G., Bell, T.G., Christensen, K.H., Saltzman, E.S., Miller, S.D., Ward, B., 2017. Parameterizing air–sea gas transfer velocity with dissipation. *J. Geophys. Res.: Oceans* 122 (4), 3041–3056.

Friedlingstein, P., Jones, M., O’sullivan, M., Andrew, R., Hauck, J., Peters, G., Peters, W., Pongratz, J., Sitch, S., Le Quéré, C., et al., 2019. Global carbon budget 2019. *Earth Syst. Sci. Data* 11 (4), 1783–1838.

Gattuso, J.P., Frankignoulle, M., Wollast, R., 1998. Carbon and carbonate metabolism in coastal aquatic ecosystems. *Annu. Rev. Ecol. Syst.* 29 (1), 405–434.

Harrison, E.L., Veron, F., Ho, D.T., Reid, M.C., Orton, P., McGillis, W.R., 2012. Nonlinear interaction between rain- and wind-induced air–water gas exchange. *J. Geophys. Res.: Oceans* 117 (C3).

Hersbach, H., Bell, B., Berrisford, P., Hirahara, S., Horányi, A., Muñoz-Sabater, J., Nicolas, J., Peubey, C., Radu, R., Schepers, D., et al., 2020. The ERA5 global reanalysis. *Q. J. R. Meteorol. Soc.* 146 (730), 1999–2049.

Ho, D.T., Law, C.S., Smith, M.J., Schlosser, P., Harvey, M., Hill, P., 2006. Measurements of air–sea gas exchange at high wind speeds in the Southern Ocean: Implications for global parameterizations. *Geophys. Res. Lett.* 33 (16).

Holding, T., Ashton, I.G., Shutler, J.D., Land, P.E., Nightingale, P.D., Rees, A.P., Brown, I., Piolle, J.-F., Kock, A., Bange, H.W., et al., 2019. The FluxEngine Air–Sea Gas Flux Toolbox: Simplified Interface and Extensions for in Situ Analyses and Multiple Sparingly Soluble Gases. European Geosciences Union (EGU)/Copernicus Publications.

Jeffery, C., Woolf, D., Robinson, I., Donlon, C., 2007. One-dimensional modelling of convective CO<sub>2</sub> exchange in the Tropical Atlantic. *Ocean Model.* 19 (3–4), 161–182.

Kuliński, K., Pempkowiak, J., 2011. The carbon budget of the Baltic Sea. *Biogeosciences* 8 (11), 3219–3230.

Laruelle, G.G., Dürr, H.H., Slomp, C.P., Borges, A.V., 2010. Evaluation of sinks and sources of CO<sub>2</sub> in the global coastal ocean using a spatially-explicit typology of estuaries and continental shelves. *Geophys. Res. Lett.* 37 (15).

Le Quéré, C., Andrew, R.M., Friedlingstein, P., Sitch, S., Pongratz, J., Manning, A.C., Korsbakken, J.I., Peters, G.P., Canadell, J.G., Jackson, R.B., et al., 2017. Global carbon budget 2017. *Earth Syst. Sci. Data Discuss.* 1–79.

- Lee, K., Sabine, C.L., Tanhua, T., Kim, T.-W., Feely, R.A., Kim, H.-C., 2011. Roles of marginal seas in absorbing and storing fossil fuel CO<sub>2</sub>. *Energy Environ. Sci.* 4 (4), 1133–1146.
- Legge, O., Johnson, M., Hicks, N., Jickells, T., Diesing, M., Aldridge, J., Andrews, J., Artioli, Y., Bakker, D.C., Burrows, M.T., et al., 2020. Carbon on the northwest European shelf: Contemporary budget and future influences. *Front. Mar. Sci.* 7, 143.
- Löffler, A., Schneider, B., Perttilä, M., Rehder, G., 2012. Air–sea CO<sub>2</sub> exchange in the Gulf of Bothnia, Baltic Sea. *Cont. Shelf Res.* 37, 46–56.
- McGillis, W.R., Edson, J.B., Hare, J.E., Fairall, C.W., 2001. Direct covariance air–sea CO<sub>2</sub> fluxes. *J. Geophys. Res.: Oceans* 106 (C8), 16729–16745.
- Meier, H.E.M., Rutgersson, A., Reckermann, M., 2014. An earth system science program for the Baltic Sea region. *EOS Trans. Am. Geophys. Union* 95 (13), 109–110.
- Nightingale, P.D., Malin, G., Law, C.S., Watson, A.J., Liss, P.S., Liddicoat, M.I., Boutin, J., Upstill-Goddard, R.C., 2000. In situ evaluation of air–sea gas exchange parameterizations using novel conservative and volatile tracers. *Glob. Biogeochem. Cycles* 14 (1), 373–387.
- Norman, M., Parampil, S.R., Rutgersson, A., Sahlée, E., 2013a. Influence of coastal upwelling on the air–sea gas exchange of CO<sub>2</sub> in a Baltic Sea Basin. *Tellus B: Chem. Phys. Meteorol.* 65 (1), 21831.
- Norman, M., Rutgersson, A., Sahlée, E., 2013b. Impact of improved air–sea gas transfer velocity on fluxes and water chemistry in a Baltic Sea model. *J. Mar. Syst.* 111, 175–188.
- Omstedt, A., Gustafsson, E., Wesslander, K., 2009. Modelling the uptake and release of carbon dioxide in the Baltic Sea surface water. *Cont. Shelf Res.* 29 (7), 870–885.
- Parard, G., Charantonis, A.A., Rutgersson, A., 2014. Remote sensing algorithm for sea surface CO<sub>2</sub> in the Baltic Sea. *Biogeosci. Discuss.* 11, 12255–12294.
- Parard, G., Charantonis, A.A., Rutgersson, A., 2015. Remote sensing the sea surface CO<sub>2</sub> of the Baltic Sea using the SOMLO methodology. *Biogeosciences* 12, 3369–3384.
- Parard, G., Charantonis, A.A., Rutgersson, A., 2016. Using satellite data to estimate partial pressure of CO<sub>2</sub> in the Baltic Sea. *J. Geophys. Res.: Biogeosci.* 121 (3), 1002–1015.
- Parard, G., Rutgersson, A., Parampil, S.R., Charantonis, A.A., 2017. The potential of using remote sensing data to estimate air–sea CO<sub>2</sub> exchange in the Baltic Sea. *Earth Syst. Dyn.* 8 (4), 1093–1106.
- Pereira, R., Ashton, I., Sabbaghzadeh, B., Shutler, J.D., Upstill-Goddard, R.C., 2018. Reduced air–sea CO<sub>2</sub> exchange in the Atlantic Ocean due to biological surfactants. *Nat. Geosci.* 11 (7), 492–496.
- Pereira, R., Schneider-Zapp, K., Upstill-Goddard, R., 2016. Surfactant control of gas transfer velocity along an offshore coastal transect: results from a laboratory gas exchange tank. *Biogeosciences* 13 (13), 3981–3989.
- Roobaert, A., Laruelle, G.G., Landschützer, P., Gruber, N., Chou, L., Regnier, P., 2019. The spatiotemporal dynamics of the sources and sinks of CO<sub>2</sub> in the global coastal ocean. *Glob. Biogeochem. Cycles* 33 (12), 1693–1714.
- Rutgersson, A., Norman, M., Åström, G., 2009. Atmospheric CO<sub>2</sub> variation over the Baltic Sea and the impact on air–sea exchange. *Boreal Environ. Res.* 14 (1), 238–249.
- Rutgersson, A., Norman, M., Schneider, B., Pettersson, H., Sahlée, E., 2008. The annual cycle of carbon dioxide and parameters influencing the air–sea carbon exchange in the Baltic Proper. *J. Mar. Syst.* 74 (1–2), 381–394.
- Rutgersson, A., Smedman, A.S., 2010. Enhanced air–sea CO<sub>2</sub> transfer due to water-side convection. *J. Mar. Syst.* 80 (1–2), 125–134.
- Rutgersson, A., Smedman, A.S., Sahlée, E., 2011. Oceanic convective mixing and the impact on air–sea gas transfer velocity. *Geophys. Res. Lett.* 38 (2).
- Sasse, T.P., McNeil, B.I., Abramowitz, G., 2013. A novel method for diagnosing seasonal to inter-annual surface ocean carbon dynamics from bottle data using neural networks. *Biogeosciences* 10 (6), 4319.
- Schernewski, G., Wielgat, M., 2004. Towards a typology for the Baltic Sea. *Manag. Baltic Sea. Coastline Rep.* 2, 35–52.
- Schneider, B., Gustafsson, E., Sadkowiak, B., 2014. Control of the mid-summer net community production and nitrogen fixation in the central Baltic Sea: An approach based on pCO<sub>2</sub> measurements on a cargo ship. *J. Mar. Syst.* 136, 1–9.
- Schneider, B., Müller, J.D., 2018. *Biogeochemical Transformations in the Baltic Sea*. Springer.
- Schneider, B., Nausch, G., Nagel, K., Wasmund, N., 2003. The surface water CO<sub>2</sub> budget for the Baltic Proper: a new way to determine nitrogen fixation. *J. Mar. Syst.* 42 (1–2), 53–64.
- Seifert, T., Tauber, F., Kayser, B., 2001. A high resolution spherical grid topography of the Baltic Sea—revised edition. In: *Proceedings of the Baltic Sea Science Congress, Stockholm*. pp. 25–29.
- Shutler, J.D., Land, P.E., Piolle, J.-F., Woolf, D.K., Goddijn-Murphy, L., Paul, F., Girard-Ardhuin, F., Chapron, B., Donlon, C.J., 2016. FluxEngine: A flexible processing system for calculating atmosphere–ocean carbon dioxide gas fluxes and climatologies. *J. Atmos. Ocean. Technol.* 33 (4), 741–756.
- Shutler, J.D., Wanninkhof, R., Nightingale, P.D., Woolf, D.K., Bakker, D.C., Watson, A., Ashton, I., Holding, T., Chapron, B., Quilfen, Y., et al., 2019. Satellites will address critical science priorities for quantifying ocean carbon. *Front. Ecol. Environ.* 18 (1), 27–35.
- Takahashi, T., Sutherland, S.C., Wanninkhof, R., Sweeney, C., Feely, R.A., Chipman, D.W., Hales, B., Friederich, G., Chavez, F., Sabine, C., et al., 2009. Climatological mean and decadal change in surface ocean pCO<sub>2</sub>, and net sea–air CO<sub>2</sub> flux over the global oceans. *Deep Sea Res. II: Top. Stud. Oceanogr.* 56 (8–10), 554–577.
- Thomas, H., Pempkowiak, J., Wulff, F., Nagel, K., 2010. The Baltic sea. In: *Carbon and Nutrient Fluxes in Continental Margins*. Springer, pp. 334–346.
- Thomas, H., Schneider, B., 1999. The seasonal cycle of carbon dioxide in Baltic Sea surface waters. *J. Mar. Syst.* 22 (1), 53–67.
- Von Schuckmann, K., Le Traon, P.-Y., Alvarez-Fanjul, E., Axell, L., Balmaseda, M., Breivik, L.-A., Brewin, R.J.W., Bricaud, C., Drevillon, M., Drillet, Y., et al., 2016. The copernicus marine environment monitoring service ocean state report. *J. Oper. Oceanogr.* 9 (sup2), s235–s320.
- Wanninkhof, R., 2014. Relationship between wind speed and gas exchange over the ocean revisited. *Limnol. Oceanogr.: Methods* 12 (6), 351–362.
- Wanninkhof, R., McGillis, W.R., 1999. A cubic relationship between air–sea CO<sub>2</sub> exchange and wind speed. *Geophys. Res. Lett.* 26 (13), 1889–1892.
- Watson, A.J., Schuster, U., Shutler, J.D., Holding, T., Ashton, I.G., Landschützer, P., Woolf, D.K., Goddijn-Murphy, L., 2020. Revised estimates of ocean–atmosphere CO<sub>2</sub> flux are consistent with ocean carbon inventory. *Nature Commun.* 11 (1), 1–6.
- Weiss, A., Kuss, J., Peters, G., Schneider, B., 2007. Evaluating transfer velocity–wind speed relationship using a long-term series of direct eddy correlation CO<sub>2</sub> flux measurements. *J. Mar. Syst.* 66 (1–4), 130–139.
- Wesslander, K., Omstedt, A., Schneider, B., 2010. Inter-annual and seasonal variations in the air–sea CO<sub>2</sub> balance in the central Baltic Sea and the Kattegat. *Cont. Shelf Res.* 30 (14), 1511–1521.
- Woolf, D.K., Land, P.E., Shutler, J.D., Goddijn-Murphy, L., Donlon, C.J., 2016. On the calculation of air–sea fluxes of CO<sub>2</sub> in the presence of temperature and salinity gradients. *J. Geophys. Res.: Oceans* 121 (2), 1229–1248.
- Woolf, D.K., Shutler, J.D., Goddijn-Murphy, L., Watson, A.J., Chapron, B., Nightingale, P.D., Donlon, C.J., Piskozub, J., Yelland, M.J., Ashton, I., et al., 2019. Key uncertainties in the recent air–sea flux of CO<sub>2</sub>. *Glob. Biogeochem. Cycles*.
- Xie, P., Arkin, P.A., 1997. Global precipitation: A 17-year monthly analysis based on gauge observations, satellite estimates, and numerical model outputs. *Bull. Am. Meteorol. Soc.* 78 (11), 2539–2558.